

2021

Exploration of protective pathways in liver disease

<https://hdl.handle.net/2144/43473>

"Downloaded from OpenBU. Boston University's institutional repository."

BOSTON UNIVERSITY
SCHOOL OF MEDICINE

Thesis

EXPLORATION OF PROTECTIVE PATHWAYS IN LIVER DISEASE

by

TALHA WAHID

B.B.A., Southern Methodist University, 2019
B.S., Southern Methodist University, 2019

Submitted in partial fulfillment of the
requirements for the degree of
Master of Science

2021

Approved by

First Reader

Zhen Y. Jiang, M.D.,Ph.D.
Associate Professor of Pharmacology & Experimental Therapeutics

Second Reader

Qiong L. Zhou, Ph.D.
Research Assistant Professor of Pharmacology

ACKNOWLEDGMENTS

I would like to express my deepest thanks to Dr. Zhen Jiang for granting me the opportunity to work in his lab, supervising and guiding my thesis project, deepening my understanding of the subject matter, and for offering a conducive work environment.

I would like to express my gratitude to Dr. Qiong Zhou for guiding me throughout my early training, teaching me proper lab techniques, and for aiding in the development of my thesis.

I would like to give thanks to my parents, Faisal and Samina Wahid for their support throughout my project. Their emotional support gave me the capacity to overcome any difficulties I encountered with my project.

EXPLORATION OF PROTECTIVE PATHWAYS IN LIVER DISEASE

TALHA WAHID

ABSTRACT

Obesity is increasing worldwide. The addition of excess calorie intake and unhealthy human behavior leads to also other diseases such as metabolic syndromes and liver disease such as non-alcoholic fatty liver disease. Furthermore, the accumulation of fat triggers specific mechanisms that, if prolonged, can cause tissue damage. For instance, the innate immune system becomes agitated in patients with NAFLD or obesity due to excessive fat accumulation. This leads to inflammation in specific tissues and infiltration of other immune cells. One of the main immune cells are neutrophils, which secrete a protease enzyme called protease neutrophil elastase. Interestingly, there have been studies conducted that have shown that when neutrophil elastase is knocked out in mouse models that mimic NAFLD, there seems to be a protective effect occurring in the body and lessen tissue scarring. A possible explanation, and the aim of this thesis, is to explore if autophagy is regulated and thus plays a role in protecting liver from inflammation and fibrosis. Western blotting approach was used to test this hypothesis. The protein samples that are used are extracted from neutrophil elastase knockout mice that have been fed a high-fat high-fructose diet and compare them to samples from wild-type control mice that have been fed a normal chow diet, high-fat diet, and high fat high fructose diet. The results indicated that potential upregulation of the autophagy pathway in the liver of neutrophil elastase knockout mice and more studies would need before accurately and

reliably acknowledging the alternation of the autophagy pathway in the liver from mouse model of NAFLD and when neutrophil elastase is knocked out.

TABLE OF CONTENTS

ACKNOWLEDGMENTS.....	iv
ABSTRACT.....	v
TABLE OF CONTENTS.....	vii
LIST OF TABLES.....	ix
LIST OF FIGURES.....	x
LIST OF ABBREVIATIONS.....	xi
INTRODUCTION.....	1
Development of NAFLD.....	2
Liver Inflammation Response.....	5
Autophagy.....	6
Autophagy Mechanism.....	8
Autophagy Pathway.....	8
Mitophagy in Liver Disease.....	13
Lipophagy in Liver Disease.....	14
Apoptosis in Liver Disease.....	15
METHODS.....	17

Small Western Blot Gels	17
Big Western Blot Gels	18
RESULTS.....	25
DISCUSSION.....	36
Limitations	37
Future Directions	38
REFERENCES.....	40
CURRICULUM VITAE.....	48

LIST OF TABLES

Table	Title	Page
1	One 10mL 8% resolving gel solution	18
2	One 17 mL for 5% and 15% resolving gel solutions	19
3	Stacking gel solution for one big gel or two small gels.	20

LIST OF FIGURES

Figure	Title	Page
1	Autophagy Pathway	10
2	p-ULK1 and ULK1 Western Blot Data	26
3	p-ATG14 and ATG14 Western Blot Data	28
4	LC3-I and LC3-II Western Blot Data	32
5	ATG5 Data Western Blot Data	34
6	Vimentin Western Blot Data	35

LIST OF ABBREVIATIONS

AMPK	AMP-Activated Protein Kinase
ATF6	Activation of Transcription Factor 6
ATG	Autophagy Related Proteins
ATP	Adenosine Triphosphate
AVG	Average
BMI	Body Mass Index
CK-18	Cytokeratin-18
CLEAR	Coordinated Lysosomal Expression and Regulation
CMA	Chaperone-Mediated Autophagy
CVD	Cardiovascular Disease
ECL	Enhance Chemiluminescent
ECM	Extracellular Matrix
ER	Endoplasmic Reticulum
GAP	GTPase Activating Protein
GRO	Growth-Related Oncogene
HFD	High Fat Diet
HFHFD	High Fat High Fructose Diet
HSC	Hepatic Stellate Cells
IL	Interleukin
IRE1	Inositol-Requiring Enzyme 1

LAL	Lysosomal Acid Lipase
LAMP-2A	Lysosomal-Associated Membrane Protein 2A
LC3	Light Chain 3
LD	Lipid Droplet
MDB	Mallory-Denk Body
MPO	Myeloperoxidase
MPP	Matrix Processing Peptidase
MTOC	Microtubule Organizing Center
mTOR	Mammalian Targets of Rapamycin
NAFLD	Non-Alcoholic Fatty Liver Disease
NASH	Non-Alcoholic Steatohepatitis
NCD	Normal Control Diet
NE	Neutrophil Elastase
NEKO	Neutrophil Elastase Knockout
NF κ β	Nuclear Factor- κ β
OMM	Outer Mitochondrial Membrane
OXPPOS	Oxidative Phosphorylation
P	Phosphorylated
PARL	Presenilin-Associated Rhomboid-Like
PE	Phosphatidylethanolamine
PERK	Protein Kinase-like ER Eukaryotic Initiation Factor-2 α Kinase
PI3K	Phosphatidylinositol-3-OH Kinase

PI3P	Phosphatidylinositol 3-Phosphate
PINK1	Phosphatase and Tensin Homolog-Induced Putative Kinase 1
P-Value	Probability-Value
RB1CC1	RB1-Inducible Coiled-Coil 1
ROS	Reactive Oxygen Species
SIRT1	Sirtuin1
STK	Serine/Threonine Protein Kinase
SQSTM1	Sequestosome-1
T	Total Protein Level
TBST	Tris-Buffered Saline with Tween
TCA	Tricarboxylic Acid
TFEB	Transcription Factor EB
TSC	Tuberous Sclerosis Complex
ULK	Unc-51 Like Kinase
VDAC	Voltage-Dependent Anion Channel
VPS	Vacuolar Sorting Protein
WT	Wild Type

INTRODUCTION

Obesity is a disease that is associated with large amounts of body fat and is defined by a person's Body Mass Index (BMI). BMI is a measurement tool based on a person's weight and height, and a person is classified as obese when the BMI is greater than or equal to 30 kg/m^2 ^[1]. There are many causes for obesity such as: genetic, behavioral, metabolic, and hormonal influences but at the core of obesity is that there is intake of more calories than there are calories that are burned off. Hence, the excess calories are stored as fat ^[2]. This disease has become prevalent all across the globe, especially in the West, due to fast food and high-calorie beverages. In 2016, more than 650 million people who are 18 years and older were obese in the world ^[3]. This trend is predicted to increase. In fact, obesity levels in America alone will continue to rise for another 40 years before reaching a plateau at which 42% of adults in America will be obese ^[4]. The risk of increasing obesity in the U.S. and around the world, is that other diseases associated with obesity will also increase. For instance, obesity is a risk for the development of non-alcoholic fatty liver disease (NAFLD). NAFLD refers to fatty liver, also known as hepatic steatosis, and it is defined by excessive fat accumulation in the absence of high alcohol consumption. This has become a serious issue and more than 83.1 million people in the United States are diagnosed with NAFLD ^[5]. The excess fat and high calorie diet associated with NAFLD puts people more at risk to develop insulin resistance and systemic inflammation. Without insulin being able to properly function in the body, more insulin needs to be produced in order to maintain normal blood glucose levels, which is the first step in developing diabetes ^[6].

Furthermore, the reason why NAFLD occurs is because of the imbalance between lipogenesis and lipolysis, which is regulated by the mitochondria. There are many mitochondria in the liver parenchyma cells and the major purpose of the mitochondria is to produce adenosine triphosphate (ATP) through oxidative phosphorylation (OXPHOS) [7]. Mitochondria is also a major site for reactive oxygen species (ROS) and regulates apoptosis. So similar to other metabolic syndromes, in NAFLD, the hepatic mitochondria are altered [8]. Additionally, the progression of NAFLD leads to nonalcoholic steatohepatitis (NASH). NASH is associated with hepatocyte inflammation and can lead to liver cirrhosis or liver scarring. Liver scarring is due to damage to hepatocytes and causes major hindrance to important liver functions. Further progression in the spectrum of NAFLDs is hepatocellular carcinoma [9]. NASH is also a component of metabolic syndromes such as obesity and type 2 diabetes. As mentioned before, a common feature of these metabolic syndromes is insulin resistance.

Development of NAFLD

To further explore the development of NAFLD, it is important to understand that the liver plays an important role to ensure the human body remains healthy through various functions such as: detoxification, biosynthesis, and metabolism of substances. Likewise, the liver is constantly exposed to substances that can induce an immune response due to bacterial products, toxins, and food derived antigens. Therefore, if the liver is damaged or inflamed it can cause many clinical complications. One of the clinical complications that result from chronic damage to the liver is fibrosis, which is the result

of excessive accumulation of extracellular matrix (ECM) proteins such as collagen. This, in fact, is a characteristic of most types of chronic liver diseases ^[10]. If the liver gets further damaged, the liver fibrosis can result in cirrhosis, which produces hepatocellular dysfunction and increased intrahepatic resistance to blood flow. This results in hepatic insufficiency and portal hypertension, which at that point a liver transplant would be needed.

Luckily, after an acute injury, the liver is able to return to normal function after proliferation and remodeling of the remaining cells. This is helped through the interaction of innate immune liver cells such Kupffer cells, dendritic cells, neutrophils, and innate-like lymphocytes with parenchymal cells (i.e. hepatocytes and liver sinusoidal endothelial cells) ^[11]. This is a normal response and is followed by an inflammatory response and limited deposition of ECM. However, if this injury is chronic, continues for a longer period of time, the liver eventually will fail to respond by regenerating cells. Instead, this can lead to parenchymal scarring and organ failure by the activation of hepatic stellate cells (HSCs), which is characteristic of liver cirrhosis ^[12]. As mentioned before, many metabolic diseases are caused by overnutrition and in the case of NAFLD, high calorie intake leads to insulin resistance. This decreases the antilipolytic effect on adipose tissue; therefore, there is more breakdown of triglycerides. With the increase of breaking down stored fat, there is more circulation of free fatty acids and glycerol. With an increase in free fatty acids, there is higher uptake of free fatty acids by the liver, which leads to increase accumulation of lipids in hepatocytes ^[13]. Additionally, dysfunctional adipose tissue lowers production of adiponectin, which is hormone that regulates fatty acid

breakdown, and there is an increase in adipokines released such as leptin leading a low-grade pro-inflammatory state ^[14].

Although not all dietary lipids have cytotoxic effects, accumulation of toxic lipids in the liver is correlated with organelle dysfunction, specifically the endoplasmic reticulum (ER) and mitochondria. This is known as lipotoxicity. The result of lipotoxicity related to ER stress, which is caused by deregulation in its reaction to misfolded proteins and response of intracellular pathways of the ER ^[15]. One of the pathways involves the overactivation of RNA-dependent protein kinase-like ER eukaryotic initiation factor-2 α kinase (PERK) and activation of transcription factor 6 (ATF6). This pathway leads to more secretion of pro-inflammatory cytokines via nuclear factor- κ B (NF κ B) pathway. The other pathway of the ER is involved is called inositol-requiring enzyme 1 (IRE1), which helps release proinflammatory cytokines as well ^[16].

There is also mitochondrial stress that is caused by lipotoxicity, but this leads to increased acetyl-CoA synthesis, which is important for the tricarboxylic acid (TCA) cycle. The TCA cycle occurs in the mitochondrial matrix. The disruption of the normal TCA cycle function increases reactive oxygen species (ROS) formation ^[17]. Also, since β -oxidation happens in the mitochondrial matrix, mitochondrial stress also alters this process and leads to formation of toxic lipid intermediates like ceramides ^[18].

With the combination of lipotoxicity and inflammation established in NAFLD, there will be an immune response to activate the innate immune cells to lessen the inflammation and repair the damage. However, too much response by immune cells can lead to the development of NASH.

Liver Inflammatory Response

It has been known that obesity can lead to the progression of NAFLD and insulin resistance. The augmented levels of free fatty acids in the liver and adipose tissue leads to activation of inflammatory pathways that are related to activation and attraction of the immune system. For instance, neutrophils recruited to the liver are mediated by interleukin (IL) – 8 and growth-related oncogene (GRO) alpha ^[19]. Although neutrophils are initially entering the inflamed site to help alleviate damage, increased infiltration of neutrophils can lead to severe stages of NAFLD, such as: NASH and cirrhosis.

The damage to the liver by neutrophils can be related to two enzymes that are associated with neutrophils. One of the enzymes is called myeloperoxidase (MPO). Since MPOs are expressed in neutrophils, they are as used as a neutrophil marker in many studies. MPOs can further damage sites of inflammation by reacting with hydrogen peroxide to form oxidizing species like hypochlorous acid/hypochlorite ^[20]. The oxidizing species can damage biological substrates, such as: DNA, lipids, and protein amino groups. MPOs have also been found in a subtype of Kupffer cells, which are liver macrophages. A study found that MPOs that contain a specific kind of macrophage, M1, could play a role in NAFLD since M1 macrophages were prevalent in obese adipose tissues ^[21]. Therefore, M1 macrophages are associated with obesity and insulin resistance. M1 macrophages are known to produce reactive oxygen and nitrogen species ^[22].

Neutrophils also secrete neutrophil elastase (NE). This protease is released in response to inflammation and promotes enhancing the chronic inflammatory state ^[23]. A recent study demonstrated that obese mice that had a deletion of NE causes a reduction in

tissue inflammation and was associated with decreased adipose tissue neutrophil and macrophage levels [24, 25]. The results also indicated that there was improved glucose tolerance and increased insulin sensitivity. Both MPO and NE genes were shown to be elevated obese patients and is also associated with BMI and markers of cardiovascular disease (CVD) [26]. Likewise, the improved function of bodily function after NE was knocked out, could be explained by the upregulation of autophagy.

Autophagy

Autophagy derives from the Greek language, where “auto” means self and “phagy” means eating [27]. Therefore, autophagy is a “self-eating” mechanism. The autophagy process removes materials that are not functional via lysosomal degradation in cells in order to produce nutrients and energy for the maintenance of cellular homeostasis [28]. For example, autophagy would clear cells of misfolded proteins and damaged organelles such as the mitochondria. In addition to removal of material, autophagy also plays a role in promoting cellular senescence, protects against genome instability, and prevents necrosis. Autophagy is activated by stresses that occur such as nutrient starvation, organelle damage, protein misfolding, and pathogen infection [29]. Therefore, without the autophagy process, many diseases can ensue such as diabetes, liver diseases, and autoimmune diseases.

Autophagy can either be non-selective or selective. For instance, mitophagy is a selective autophagy for the mitochondria. Mitophagy is a specific kind of process and subset of a broader mechanism called “organellophagy”, which eliminates damaged

organelles and induces the promotion of new organelles. Therefore, mitophagy clears damaged mitochondria and promotes new ones to be made ^[30]. Mitophagy and other specific kinds of autophagy will be discussed further later in the thesis.

There are three types of autophagy: macroautophagy, micro-autophagy, and chaperone-mediated autophagy (CMA). These all promote proteolytic degradation of cytosolic components at the lysosome. Macroautophagy, which is typically referred to as “autophagy” in most papers, involves an autophagosome, which is a double membrane-bound vesicle, from the cytoplasm to the lysosome ^[31]. Macroautophagy serves as the guardian of human health because it is triggered when there is nutrient starvation, damaged organelles, aggregated protein, and infections so that the cells can be saved from harmful effects and can maintain homeostasis ^[32]. The second type of autophagy is called microautophagy. Microautophagy is a process that allows for cytosolic components to be taken up by the lysosome via rearrangement and invagination of the lysosomal membrane into the lumen ^[33]. Both macro- and micro-autophagy are able to engulf large structures through both selective and non-selective mechanisms. The third type of autophagy is CMA. This is a process that allows for materials to be degraded by recognizing substrates that contain the pentapeptide “Lys-Phe-Glu-Arg-Gln” (KFERQ) by a chaperone protein, such as Hsc-70, and translocate these substrates into the lumen of lysosomes through docking of lysosomal membrane receptor lysosomal-associated membrane protein 2A (LAMP-2A) resulting in their unfolding and degradation ^[34].

Autophagy Mechanism

The process of autophagy starts with the rearrangement of the membrane for nucleation of the phagophore ^[35]. An isolation membrane or phagophore is derived from various organelles such as the ER, trans-Golgi, mitochondria, plasma membrane, and endosomes ^[36]. The cup-shaped phagophore then elongates and matures into a double-membraned autophagosome ^[37]. The autophagosomes, which now have enclosed substances that will be degraded, mature through fusion with the lysosome, thus leading to the degradation of autophagosomal contents by lysosomal acid proteases. There are permeases and transporters that let amino acids and other by products of degradation back out to the cytoplasm, where they can be re-used for building macromolecules and for metabolism. Therefore, the autophagy process is nick-named as a recycling process for the cell and can mediate damage control by removing non-functional proteins and organelles. This process will further be explained in depth next and can be visualized in Figure 1.

Autophagy Pathway

Autophagy related proteins (ATG) are arranged into functional complexes to initiate autophagy. In eukaryotic cells, starvation inhibits the activity of mammalian targets of rapamycin (mTOR), which is a serine/threonine protein kinase that is involved in cellular metabolism ^[38]. Therefore, when mTOR is inhibited due to starvation, this leads to translocation of the unc-51 like kinase (ULK) complex, which contains ULK1/2, ATG13, RB1-inducible coiled-coil 1 (RB1CC1 or FIP200), and ATG101, from the

cytoplasm to a membrane enclosed compartment. At the same time, the ULK complex recruits phosphatidylinositol-3-OH kinase (PI3K) complex to the nucleated domain from the ER and stimulates PI3K complex. The PI3K complex includes vacuolar sorting protein 34 (Vps34)/PI3KC3, Vps15, Beclin1, and ATG14. This promotes autophagosome synthesis. Furthermore, Vps34 is a class III PI3K and is required to generate of phosphatidylinositol 3-phosphate (PI3P) [39].

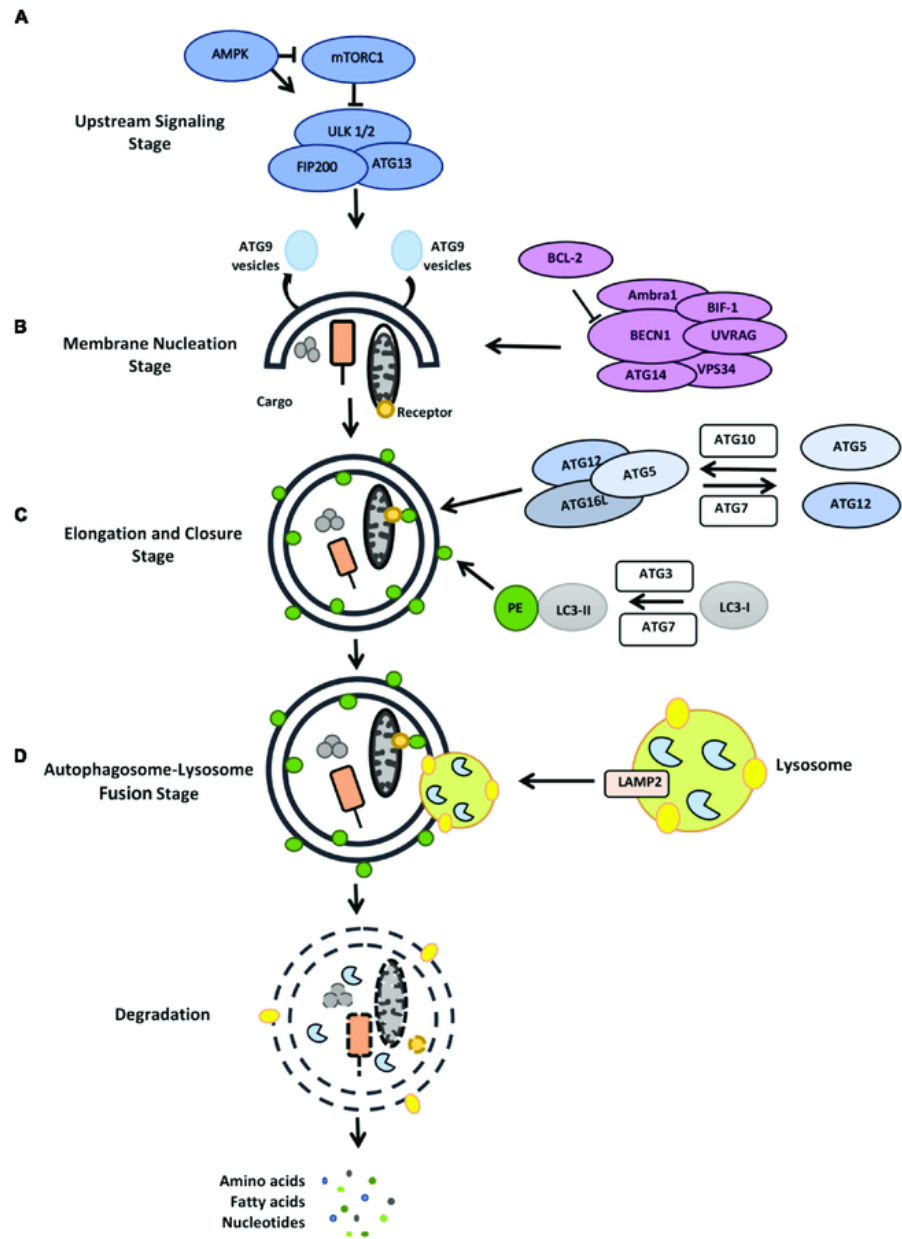


Figure 1. Autophagy Pathway^[40]

Additionally, phagophores are regulated by two ubiquitin-like conjugation system involving the generation of Atg5-Atg12-Atg16L complex and phosphatidylethanolamine

(PE)-conjugated microtubule-associated protein 1 light chain 3 (LC3) ^[41]. The first part of this pathway is that Atg7 activates Atg12, which is then transferred to Atg10. Lastly, this complex then covalently binds to Atg5. With the addition of Atg16L1, the Atg5-Atg12 forms a large complex and localizes to the phagophore. This complex, then, influences the second pathway. The second pathway involves LC3 to be synthesized as a cytosolic protein and cleaved by Atg4, which then transforms LC3 into LC3-I. LC3-I becomes LC3-II when it conjugates with PE by Atg7 and Atg3. The LC3 protein can now be recruited onto the expanding phagophore and will remain on the autophagosome for the rest of the pathway ^[42]. Along the maturation process, the autophagosomes engulf material in the cytoplasm that are to be degraded due to potential toxins or damaged substances. Autophagic substrates are also targeted for degradation by adaptors such as sequestosome-1 (SQSTM1/p62) ^[43]. Autophagosomes are then transported along the microtubule network to the microtubule organizing center (MTOC). Along the path to MTOC and before fusing with the lysosomes, autophagosomes can also fuse with endosomes to form amphisomes, which increase during starvation state ^[44]. The fusion of autophagosomes with lysosomes results in the generation of autolysosomes where degradation of material occurs, such as autophagy substrates, and amino acids are recycled to be reused.

Since mTOR plays a vital role in the regulation of autophagy, further explanation is needed. mTORC1, which contains mTOR, is one of two complexes but compared to mTORC2 complex, mTORC1 complex contains Raptor. In order to regulate mTORC1 complex, PI3K/Akt phosphorylates subunit tuberous sclerosis complex (TSC), which

consists of TSC2 and TSC1 ^[45]. The TSC2 subunit has a GTPase activating protein (GAP) domain, and when this enzyme is active it inhibits Rheb ^[46]. However, Rheb activates mTORC1 and resides on the intracellular membranes (e.g. lysosomes). So, when Rheb is inactive, mTORC1 complex is also inactive. Rheb can be activated when bound to GTP, which in turn activates mTORC1 ^[47]. Hence, when Rheb is inactive, mTOR is inactive and autophagy pathway is activated.

Autophagy can also be regulated through ATP:AMP ratio by cell homeostasis kinases such as AMP-activated protein kinase (AMPK) and serine/threonine protein kinase (STK11 or LKB1). This pathway is positively stimulated when there is low cellular energy. Furthermore, LKB1 activates autophagy through AMPK via inhibition of mTORC1 due to activation of TSC2 subunit. TSC2 is regulated by WIPI3 and FIP200; therefore, the LKB1-AMPK-TSC2 complex plays a role in autophagy induction and autophagosome formation ^[48]. AMPK can stimulate the autophagy pathway by directly phosphorylating ULK1, Vps34, and Beclin1 ^[49].

Lastly, autophagy can also be regulated at the transcription level through the regulation of the transcription factor EB (TFEB) by mTORC1 complex. TFEB stimulates the expression of genes that regulate lysosome biogenesis and autophagy by binding to coordinated lysosomal expression and regulation (CLEAR) motif in the promoter region in the nucleus of cells ^[50]. Recent research has demonstrated that phosphorylation of TFEB by mTORC1 complex inactivates TFEB under nutrient rich conditions. This phosphorylation occurrence allows for TFEB to interact with cytosolic chaperone proteins which makes TFEB to remain in the cytosol ^[51]. In starving condition, mTORC1

is inactivated and therefore allows for TFEB to translocate to the nucleus where it causes the expression of multiple lysosomal and autophagy related genes including p62 and LC3B [52].

Mitophagy in Liver Disease

Mitochondrial function and homeostasis are important in many different processes in the body. Antioxidant systems are the primary way to ensure mitochondrial function stays intact and prevent oxidative damage [53]. So, when the mitochondria or the OXPHOS complex has been damaged, they are degraded by the mitophagy pathway [54]. This pathway is widely regarded as a protective cover in the NAFLD progression.

In a healthy mitochondrion, phosphatase and tensin homolog-induced putative kinase 1 (PINK1) is degraded by the matrix processing peptidase (MPP) and the presenilin-associated rhomboid-like (PARL) protease [55]. Therefore, when the mitochondrial is depolarized, PINK1 recruits Parkin onto the outer mitochondrial membrane (OMM) [56]. One of the most studied Parkin substrates in the OMM is the voltage-dependent anion channel (VDAC), also known as mitochondria porin [57]. Therefore, when Parkin ubiquitinates VDAC, soluble autophagy receptors, such as p62, is recruited to the mitochondria [58]. These mitophagy proteins contain ubiquitin binding domain and a LC3-interacting region. Likewise, this means LC3 is involved in mitophagy. Since there are several LC3 receptors located on the mitochondria, LC3 can bind directly on the receptors and recruit autophagosomes to engulf mitochondria. In NAFLD patients, mitochondria are enlarged and swollen with a loss of cristae [59]. In

NAFLD model mice, it has been shown that PINK1 and Parkin have been significantly downregulated and associated with the activation of mitochondrial-related apoptosis [60].

Lipophagy in Liver Disease

As mentioned previously, the main feature of NAFLD is steatosis or high levels of lipids in the form of lipid droplets (LDs). And lipophagy, also known as LD autophagy, is the process responsible for lipid breakdown in the liver. The pathway starts with protein-mediated engulfment of substance (i.e. portion or whole LD) within the cytosolic double membrane of the vesicle, then there is tracking and transport of autophagosome to the lysosome where the autophagosome and lysosome fuse together to form an autophagolysosome. After the completion of the fusion, the substances that were initially sequestered are degraded by lysosomal enzymes (i.e. lipases) such as lysosomal acid lipase (LAL). LAL is active in acidic pH and mediates lysosomal degradation of triglycerides, lipoproteins, and lipids [61].

Furthermore, lipophagy begins with cytosolic LC3 (LC3-I) being conjugated to PE by Atg-7 and Atg-3 during the formation of autophagosomal membrane. This forms LC3-II. And when the autophagosome fuses with the lysosome in the last steps, LC3-II is degraded by lysosomal proteases. The degradation of LC3-II is used as a marker to show reduced autophagy since an increase of LC3-II level is connected with an impairment in the pathway [62]. Also, p62/SQSTM1 is an autophagy receptor that is required for selective macroautophagy (e.g. lipophagy) connecting polyubiquitinated cargo with autophagosomes. Therefore, p62/SQSTM1 represents another marker for autophagy. So,

if there is a buildup of this marker, it represents that the selective autophagy pathway has not been properly functioning [63].

Apoptosis in Liver Disease

Apoptosis, or programmed cell death, is a cellular mechanism that leads to cells to change morphology and eventually leads to its death. Caspases have apoptotic function. And in NASH patients, active (i.e. cleaved) caspase 3 and 7 have been strongly correlated with hepatocyte apoptosis and the progression of NASH [64]. Caspase 3 in the liver is known to cleave cytokeratin-18 (CK-18) which is a major intermediate filament protein. The generation of CK-18 is an indicator of patients with NAFLD and can lead to further progression to NASH [65]. Mallory-Denk bodies (MDBs) are also characteristic of NASH and can help distinguish between relatively benign simple steatosis and more serious progression NASH. Mice studies have shown that mice that have genetic overexpression of CK-8 and consumption of high-fat diet triggered hepatocellular injury, ballooning, apoptosis, inflammation, and MDB development [66]. Furthermore, apoptosis in the liver is associated with miR-34a/Sirtuin1 (SIRT1)/p53 signaling in NASH [67]. And the p53 and its transcriptional miR34a target have been shown to be involved in the pathogenesis of fatty liver. So, if p53 is inhibited, there has been an increase in steatosis, associated oxidative stress, and apoptosis in mice models of NAFLD [68]. Lastly, increased vimentin fragments have been found in NASH patients and indicate apoptosis in the liver as well [69].

The aim of the thesis is to investigate a possible autophagy pathway that provides a protective effect in mice models that have neutrophil elastase knocked out. It has been shown in previous studies that inhibition of neutrophil elastase results in reduction in insulin resistance but to explain why this occurs maybe due to upregulation of the autophagy pathway. Some of the other pathways being looked at as mentioned in the introduction include ER stress, mitophagy pathway, apoptosis pathway, mitochondrial makers, and fibrosis marker

METHODS

Both big and small gels of Western Blots have similar protocol, but the main contrast is the initial steps.

Small Western Blot Gels

In order to prepare small gels, two 1.5mm gel plates are rinsed and cleaned to get rid of any debris. One plate should be taller and have BIO-RAD 1.5mm written on it while the other plate should be shorter with no writing. In order to hold the two pieces of glass together, a green clamp is used with the shorter plate in the frontmost position. It is important to make sure that the sides and bottom edge of the plates are lined up prior to closing the clamp to prevent leakage. The green clamp is then placed on top of the clean rubber strip. Furthermore, to test for leaks, pipette ~0.5mL of isopropyl alcohol between the two plates. The next step is to prepare resolving gel and stacking gel solutions in two separate beakers. The amount of each substance depends on what percentage-type of gel is being run and how large the gel is. Table 1 is an example for 8% resolving gel, which is typically run for the small gels in this thesis. 7mL is usually used for each gel. It is important to note that TEMED should only be added right before the solutions are ready to be poured in between the glass pieces. Using a pipette and moving from side to side, pour water or 100% alcohol on the top of the resolving gel solution to even out the top part of the solution. The resolving gel solution will take 30 minutes to solidify. The next step will be to make stacking gel solution (Table 3). Once the solution has become solid, pour off the water or alcohol into a tissue. Choose an appropriate comb with the

appropriate number of wells, rinse it, and insert it between the two glass pieces. After making the stacking gel solution, then add TEMED to the mix and pipette the solution from one corner up the top of the glass. It is important to make sure that there are no bubbles in the solution. Lastly, wipe off the excess solution and save the remaining stacking gel solution to check when it gets.

Table 1. One 10mL 8% resolving gel solution

30 % Acrylamide	2.7 mL
Resolving Gel Buffer	2.5 mL
Water	3.8 mL
1% APS	1 mL
TEMED	12 uL

Big Western Blot Gels

In order to prepare big gels, two glass plates are rinsed and cleaned to get rid of any debris. One plate should be taller while the other plate should be shorter. In order to hold the two pieces of glass together, two white clamps are used with the shorter plate in the frontmost position. It is important to make sure that the sides and bottom edge of the plates are lined up prior to closing the clamp to prevent leakage. The whole structure is then placed on top of the clean rubber strip. Furthermore, to test for leaks, pipette 1-2 mL of isopropyl alcohol between the two plates. The next step is to prepare resolving gel and

stacking gel solutions in two separate beakers. The amount of each substance depends on what percentage-type of gel is being run and how large the gel is. Table 2 is an example of 5% and 15% gradient gel, which is typically run for the big gels in this thesis. 17mL is usually used for each gel. To mix the 5% and 15% solutions into the same gel, a mixture apparatus is needed in order to ensure that the bottom part of the gel is 15% while the top portion is 5%. It is important to note that TEMED should only be added right before the solutions are ready to be poured in between the glass pieces.

Table 2. One 17 mL for 5% and 15% resolving gel solutions

	5%	15%
30% Acrylamide	2.83 mL	8.50 mL
Resolving Gel Buffer	4.25 mL	4.25 mL
Water	9.4 mL	3.73 mL
1% APS	0.56 mL	0.56 mL
TEMED	8 uL	8 uL

Table 3. Stacking gel solution for one big gel or two small gels. This amount should provide stacking gel solution for two small gels and one big gel.

30 % Acrylamide	1.6 mL
Stacking Gel Buffer	2.5 mL
Water	3.24 mL
1% APS	0.66 mL
TEMED	15 uL

Then pipette and move from side to side. Next, pour water or 100% alcohol on the top of the resolving gel solution to even out the top part of the solution. The resolving gel solution will take one hour to solidify. The next step will be to make stacking gel solution (Table 3). Once the solution has become solid, pour off the water or alcohol into a tissue. Choose an appropriate comb with the appropriate number of wells and rinse it. After making the stacking gel solution, then add TEMED to the mix and pipette the solution from one corner up the top of the glass. Then add the comb. It is important to make sure that there are no bubbles in the solution and to wipe off the excess solution.

The remaining portion of the protocol for both small and big gels will be the same.

After the stacking gel has set, which will take about 30 minutes, the next step is to rinse the glasses with water and set them up in the appropriate running buffer container. Afterwards, gently take off the combs and pour 1x Running Buffer between the two glass plates until it reaches the top. The next step is to load the samples. Make sure prior to

loading the samples have been fully defrosted and have recorded how the gels will be loaded. Also, it important to add 1x Running Buffer in the container so that the lower portion of the glass pieces have been covered and that there are no leakages from the top of the glasses as well. Then use the tips from the blue/white box and pipette the desired amount of marker into the well. In order to prevent air bubbles when pipetting, pull the tip out of the gel when there is only a few of the sample left in the tip. This still will be repeated for all the samples and loading markers. The starting voltage for the gels can be 35V. In order to speed up the running time, the voltage can be increased. Once the samples are as close as possible to the bottom edge of the plate without spilling into the running buffer, turn off the machine.

The next part will be to transfer the samples to the nitrocellulose membrane. Grab two pieces of paper, a tray, the 1x transfer buffer, the transfer cassette with the black and white fabric, and nitrocellulose membrane. The first step will be to cut the membrane and paper to the appropriate size. For a small gel, the membrane and paper should measure 5cm x 9cm. For a big gel, it should measure 13cm x 17cm. There will be four pieces of paper (two on each side of the membrane) and one membrane will be used for one small gel. As for big gels, two pieces of paper (one for each side) and one membrane will be used. The next step will be to fill a tray halfway with the transfer buffer, carefully separate the gel from the glass plates, and place the gel in the transfer buffer. The pieces of paper will go behind the gel and then on top of the gel, the nitrocellulose membrane is placed. The remaining paper will be used to cover the membrane. It is important to use a rolling type of tool to remove all air bubbles between each layer. Afterwards carefully

transfer the layers all together onto the black and white mesh. The gel should be on the black side while the membrane should be on the white side. The black and white mesh should be put in the appropriate transfer box and in the right direction (i.e. red to red and black to black). Then 1x transfer buffer is poured into the container until the cassette is submerged. Cover the box and put it into the fridge. For two big gels, the the current is set to 400 mA for five hours while for small gels current is set the current to 400mA for one gel or 500-600mA for two gels. This process for small gels can either be ran for 2-3 hours or for overnight at 160 mA.

Once the transfer period is over, pour back the transfer buffer into its appropriate container and place the membranes on a clean glass surface to cut the membrane(s). First, remove the membrane from the transfer cassette. Cut the sides of the membrane off, leaving only a little space between the edge of the cut membrane and the protein markers. Using a pencil, write over the makers and cut the membrane into strips corresponding to the appropriate molecular weight (kDa) that the antibodies appear. It's important to write the antibody on the edge of the strip and cut the right corner off to denote the left side and right side of the membrane. Use forceps to transfer the strip into the appropriate container and make sure that the membrane doesn't dry out. Repeat these steps for all the membranes. The next step is to make 4% BSA solution for blocking, which for 300mL of blocking solution it is 300 ml of 1x TBST plus 12g (4%) of BSA powder and 0.3 grams (0.1%) of sodium azide. Once the blocking solution is made, pour the 4% of BSA solution into the container so each membrane is covered. Put the membrane on the shaker

in for thirty minutes. After thirty minutes pour out the 4% BSA solution and rinse the membranes with water.

Next, pour the desired primary antibody solution over the membrane. Put the container on the shaker in the 4° fridge for overnight. Once that step is completed, pour the primary antibody solution back in their appropriate falcon tube to be stored in the fridge for re-use. Wash the membranes with 1xTBST 3 times for 10 minutes each and then rinse the membrane with water. Then pour secondary antibodies in the appropriate container with membranes. The secondary antibody is made up of 1xTBST and secondary antibody. So for example, if the primary antibody is goat, anti-goat secondary antibody will be needed. The anti-goat secondary has a dilution of 1:10,000 and 0.1% of BSA powder needs to be added as well. As for the other secondary antibodies, the dilutions are: anti-rabbit is 1:7,500 dilution, and anti-mouse is 1:10,000 dilution. After pouring the secondary, place the membranes on shaker for 1 hour and 30 minutes. Afterwards, pour out the secondary into a sink and rinse the membranes in water. Pour 1x TBST back on to the membrane for 10 minutes for 3 times and then rinse in membrane in water.

The next step is about imaging. The first thing to do is get a cassette sheet protector and cut off the top, bottom, and left of the sheet protector. Make the ECL solution using equal amounts of stable peroxide and luminol/enhancer into a falcon tube. It is necessary to cover the falcon tube with aluminum foil to protect from light. Then place wrapping paper on a table and pipette ECL solution enough to cover each membrane. Pick up membrane, dab the membrane out on tissue to remove excess liquid,

and place the membrane face down on the plastic wrap so that the ECL solution touches side of the membrane where the sample is located. This step will need to be repeated for all membranes. After placing all membranes down, set a 3-minute timer before picking up the membrane and placing the membranes with the protein side faced-up on the sheet protector and in the proper molecular weight order. Then place the sheet protector in the cassette.

Lastly, take the cassette to the imaging room and click on ImageQuant 4000 machine icon. Then make sure the lights are off and open the cassette. Afterwards place the sheet protector into the machine. It is important to wipe the sheet protector to get rid of air bubbles that maybe around the membrane. If the bands are too dark, use a lesser exposure time. If the bands are too light, use a higher exposure time. Then finally make sure to save each membrane in a file labeled with its antibody, sample date, and exposure time.

RESULTS

Mouse models were used to demonstrate the effects of neutrophil elastase on obesity related tissue damage. The mice were split into 4 conditions. The 4 conditions were wild-type normal control diet (WT-NCD), wild-type high-fat diet (WT-HFD), wild-type high-fat high-fructose diet (WT-HFHF), and neutrophil elastase knockout mice high fat high fructose diet (NEKO-HFHF). Each experiment had between 6-7 mice. NCD mice were fed a normal chow diet pellet. HFD mice were fed a high fat diet pellet. HFHF mice were fed a high-fat and high-fructose pellet. NEKO-HFHF mice were ones that had the NE gene knocked out and were subsequently fed a high-fat high-fructose pellet.

As mentioned previously, mTOR is a master regulator of the autophagy pathway. When mTORC1 complex is activated, then autophagy is inhibited. Another master regulator is AMPK, and when this is activated so is autophagy. However, downstream both AMPK, which activates, and mTOR, which inhibits, ULK1 by phosphorylation. ULK1 is involved in initiation stages of autophagy. In figure 2, the HFD group shows significant greater intensity than the NCD group on the p-ULK1 S317 membrane. The HFHF group also shows significant greater intensity than the NCD group on the p-ULK1 S317 membrane as well. This may suggest there is upregulation of autophagy in certain diets that are high in fat or high in fat and high in fructose to provide a maintenance effect. Lastly, the NEKO-HFHF group shows significant greater intensity than the HFHF group on the p-ULK1 S317 membrane. This may point to the fact that there is a significant increase in autophagy, or at least in its initial stages, when neutrophil elastase is knocked out in diets that are high in fat and high in fructose. This aligns with

the hypothesis that there is upregulation of autophagy in NEKO-HFHFD groups in order to provide a protective effect against scarring and further progression of liver disease.

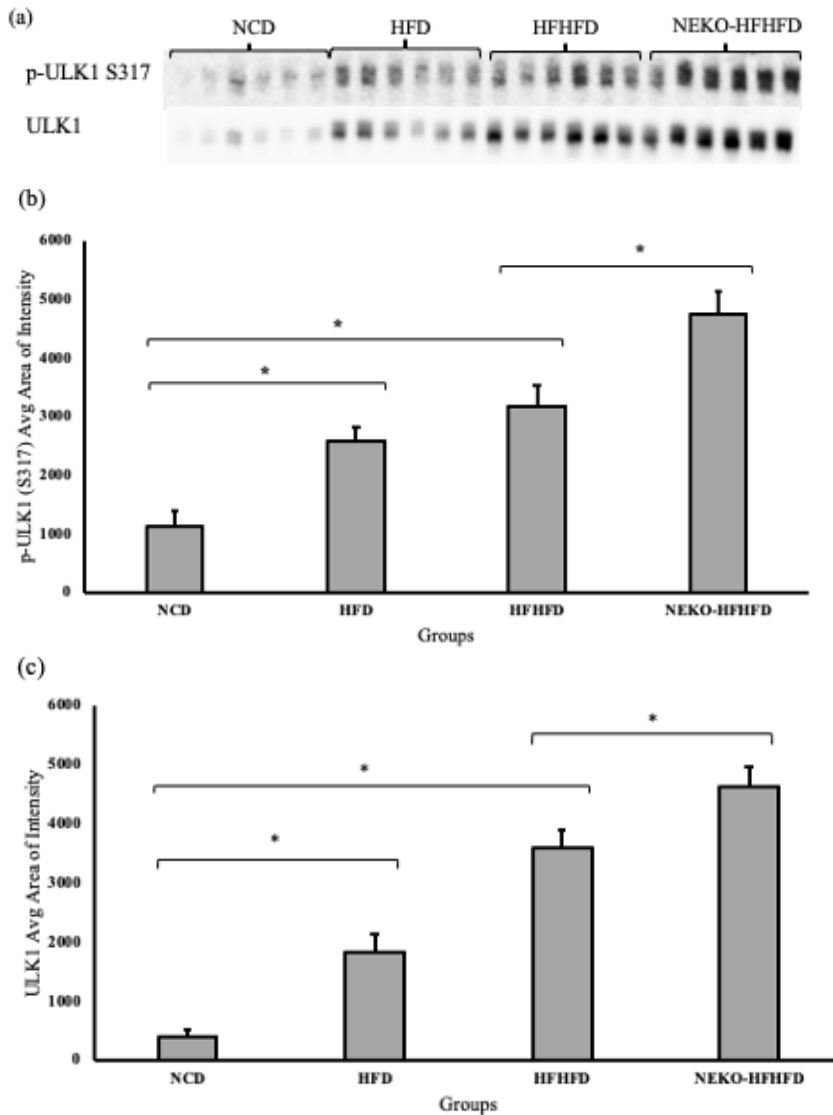


Figure 2. p-ULK1 and ULK1 Western Blot Data. 35 μ L of each sample from each group loaded onto gel. The sample groups include NCD, HFD, HFHFD, NEKO-HFHFD from mice sample collected on 07/26/19. Both primary antibodies, p-ULK1 (S317) and ULK1, are from Cell Signaling and is Rabbit antibody (1:1000 dilution). (a) top membrane shows p-ULK1 Serine 317 phosphorylation site cell signaling in the four different groups, and bottom membrane shows ULK1 protein level in the four different groups. (b) shows quantified measurement of p-ULK1 S317 band

based on average area of intensity for each group. (c) shows quantified measurement of ULK1 band based on average area intensity for each group. * $p \leq 0.05$ based on two-tailed t-test.

Also shown on figure 2, is the ULK1 membrane and its quantification. The same pattern is shown compared to its phosphorylated counterpart. The HFD and the HFHFD groups compared to the NCD group each shows significant increase of intensity. This may suggest increase of protein levels of ULK1, hence increase of autophagy markers, in diets that are high in fat or high in fat and in fructose as a maintenance effect. Lastly, the NEKO-HFHFD group has a significantly higher intensity in the ULK1 band when compared to the HFHFD group. This could mean that there is a higher protein level when neutrophil elastase is knocked out in high fat and high fructose diets. This boosts the hypothesis that there is upregulation of autophagy in NEKO-HFHFD groups in order to provide a protective effect against scarring and further progression of liver disease.

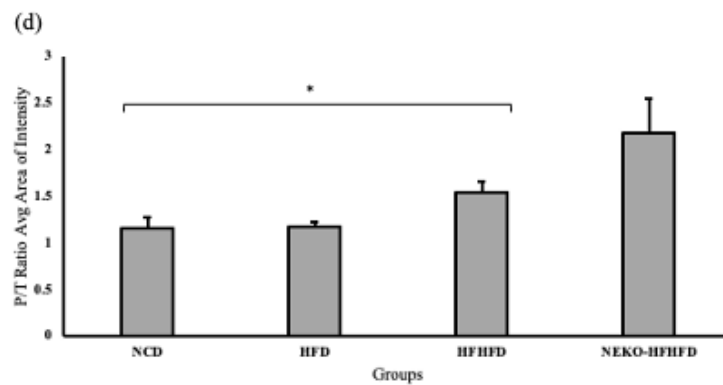
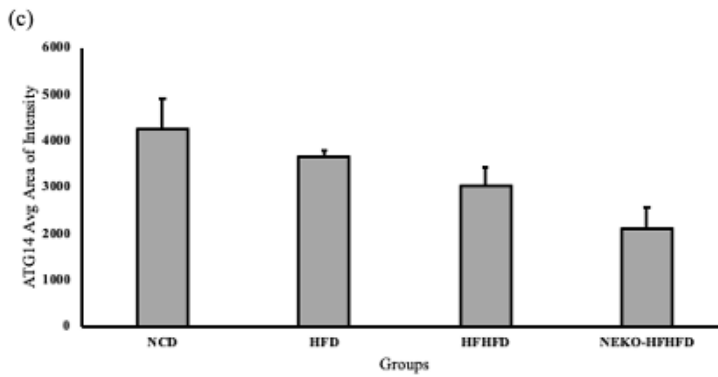
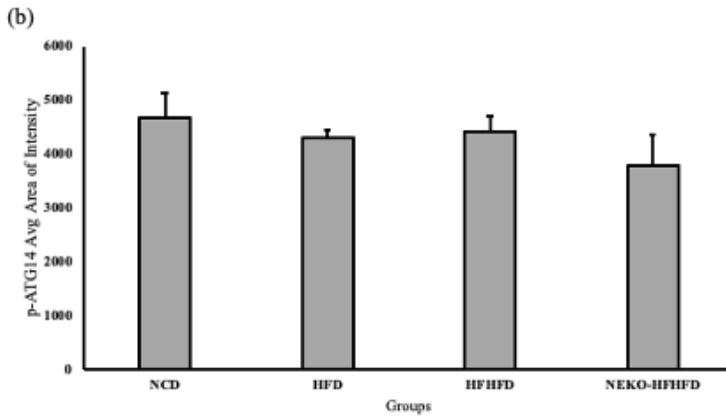
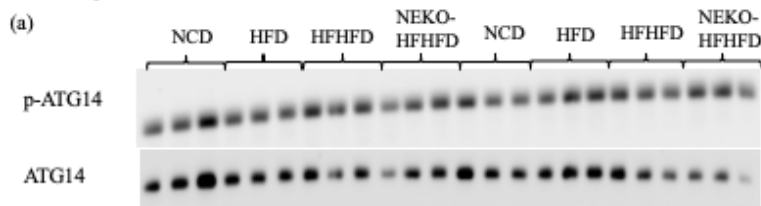


Figure 3. p-ATG14 and ATG14 Western Blot Data. 35 μ L of each sample from each group loaded onto gel. The sample groups include NCD, HFD, HFHFD, NEKO-HFHFD from mice sample collected on 07/26/19. Both primary antibodies, p-ATG14

and ATG14, are from Cell Signaling and is Rabbit antibody (1:1000 dilution). (a) top membrane shows p-ATG14 cell signaling in the four different groups, and bottom membrane shows ATG14 protein level in the four different groups. (b) shows quantified measurement of p-ATG14 band based on average area of intensity for each group. (c) shows quantified measurement of ATG14 band based on average area intensity for each group. (d) shows ratio of p-ATG14 (P) over ATG14 (T) based on average area of intensity for each group. * $p \leq 0.05$ based on two-tailed t-test.

Along with the activation of the ULK1 complex (includes ULK1, ATG101, ATG13, and FIP200), PI3K complex is also needed to be activated in order for phagophore formation to occur. The PI3K complex includes ATG14, Beclin-1, Vps34, and Vps15. ATG14 is a downstream target of ULK1. ATG14 can be activated by when it is phosphorylated by ULK1^[70]. As shown in Figure 3, the HFD group shows lesser amount of intensity than the NCD group on the p-ATG14 membrane; however, this comparison is not significant and has a p-value greater than 0.05; therefore, the data comparison suggests that there is no relationship between the two groups and is due to chance. The HFHFD group also shows lesser intensity than the NCD group on the p-ATG14 membrane as well. This may suggest, again, that there is no relationship between the two groups since the p-value is also greater than 0.05. Lastly, the NEKO-HFHFD group shows lesser amount of intensity than the HFHFD group on the p-ATG14 membrane. This data comparison is also not significant to conclude any valuable information on autophagy and whether or not it is upregulated when neutrophil elastase is knocked out. Also shown on figure 3, is the ATG14 membrane and its quantification. The same pattern is shown compared to its phosphorylated counterpart. The HFD and the HFHFD groups compared to the NCD group each shows lesser amount of intensity. Since

this data comparison is not significant (i.e. p-value greater than 0.05), this may suggest that the comparison between the groups draws no significant conclusion and that there may not be an increase of ATG14 protein levels in in diets that are high in fat or high in fat and in fructose as a maintenance effect. Lastly, the NEKO-HFHFD group has a lesser intensity in the ATG14 band when compared to the HFHFD group. This data comparison, again, is not significant and no certain conclusion can be drawn. Since the p-value is greater than 0.05 between the HFHFD and the NEKO-HFHFD group, it cannot be concluded that that PI3K pathway, at least at the protein level of ATG14, is upregulated when neutrophil elastase is knocked out in HFHFD group. Despite the lack of significance in the previous data related to p-ATG14 and ATG14, the quantified ratio of p-ATG14 and ATG14 shows a slightly different story. In fact, when looking at the P/T ratio when comparing the HFHFD group to the NCD group, there is a significant increase in the HFHFD group. This may suggest that there is more p-ATG14 occurring in the HFHFD group relative to its protein level when compared to the NCD group; therefore, this groups may experience more upregulation of autophagy. However, when comparing P/T ratio of the NCD group to the HFD group, there is no significant different so this may suggest, as previously, mentioned any real difference between the groups. Lastly, the P/T ratio of the NEKO-HFHFD group and the HFHFD group also has a p-value greater than 0.05. This means no significant difference between the groups was found and the null hypothesis is not rejected.

Furthermore, the next part of autophagy pathway is the transformation of a phagophore to an autophagosome, which involves LC3 and ATG12-ATG5-ATG16L

complex. This part of the pathway begins with LC3-I being formed when ATG4 binds with LC3. Then LC3-I and ATG4 bind with ATG7 to form LC3-II. Both LC3-I and LC3-II are shown in figure 4. LC3-I is the top band, and the bottom band is LC3-II. Furthermore, figure 4 also notes the quantification of LC3-I and LC3-II in all four groups. The HFD group shows greater amount of intensity than the NCD group on the LC3-I bands; however, this comparison is not significant and has a p-value greater than 0.05. Therefore, the data comparison suggests that there is no relationship between the two groups and is due to chance. The HFHFD group also shows greater amount of intensity than the NCD group on the LC3-I bands as well. This may suggest that there is no relationship between the two groups since the p-value is greater than 0.05. Lastly, the NEKO-HFHFD group shows greater amount of intensity than the HFHFD group on the LC3-I bands. This data comparison is also not significant to conclude any valuable information on autophagy and whether or not it is upregulated when neutrophil elastase is knocked out. Also shown on figure 4, is the LC3-II bands and its quantification. The same pattern is shown when comparing the HFD group and the NCD group. There is an increase in intensity in the HFD group but it's not significant. However, the HFHFD group compared to the NCD group is shown to be significant. The HFHFD group shows greater intensity compared to the NCD group. This may suggest a maintenance mechanism related to autophagy in the HFHFD group due to high fat and high fructose. Lastly, when comparing the NEKO-HFHFD and HFHFD group, there is a significant difference between the intensity. The NEKO group has a significantly higher intensity compared to the HFHFD group. This may suggest that there is upregulation of autophagy

pathway and autophagosome formation when neutrophil elastase is knocked in HFHFD.

This further supports the hypothesis that there is upregulation in the NEKO-HFHFD group.

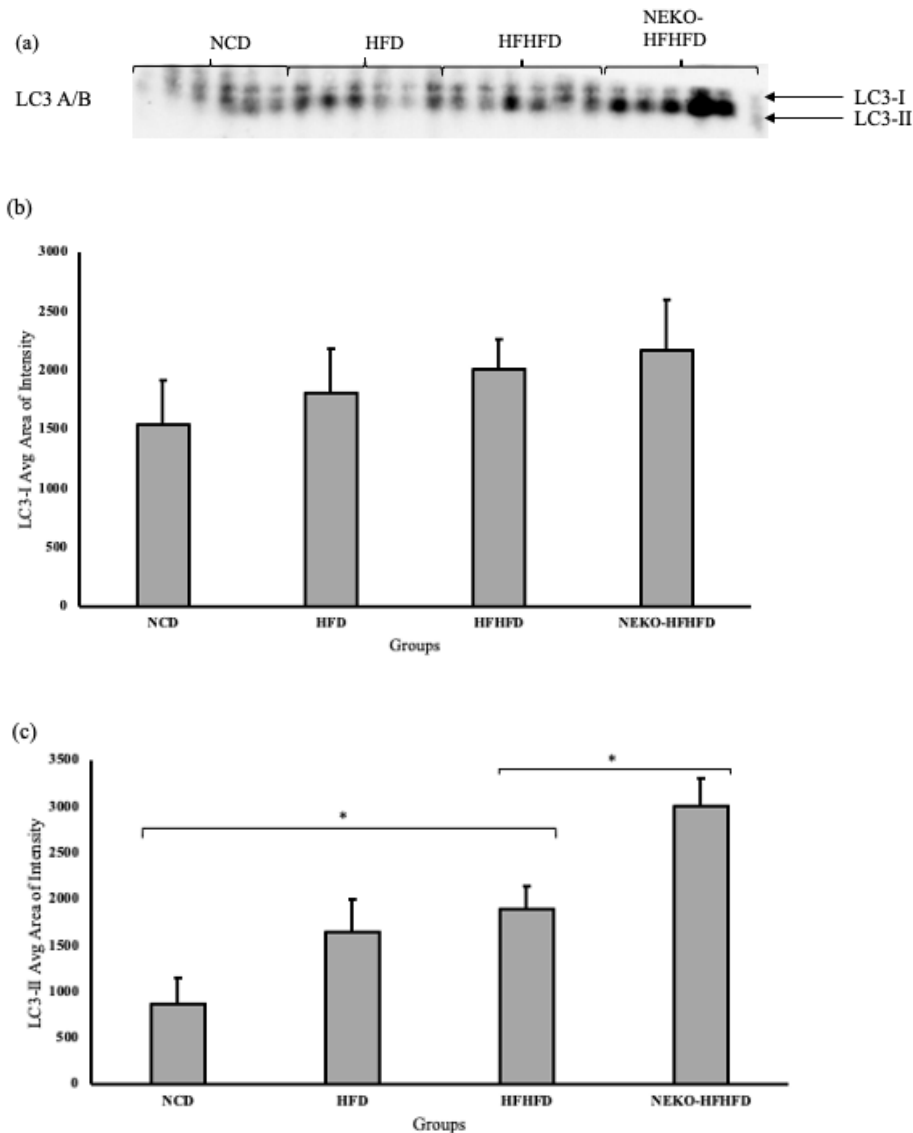


Figure 4. LC3-I and LC3-II Western Blot Data. 35 μ L of each sample from each group loaded onto gel. The sample groups include NCD, HFD, HFHFD, NEKO-HFHFD from mice sample collected on 07/26/19. Both primary antibodies, LC3-I and LC3-II, are from Cell Signaling and is Rabbit antibody (1:1000 dilution). (a) top band shows LC3-I in the four different groups, and bottom band shows LC3-II in

the four different groups. (b) shows quantified measurement of LC3-I band based on average area of intensity for each group. (c) shows quantified measurement of LC3-II band based on average area intensity for each group. * $p \leq 0.05$ based on two-tailed t-test.

Along with LC3-II being formed in order to create an autophagosome, ATG5 is also important component for that process. As mentioned previously, the transformation of a phagophore to an autophagosome, involves LC3 and ATG12-ATG5-ATG16L complex. As shown in figure 5, the HFD group shows greater amount of intensity than the NCD group on the ATG5 membrane; however, this comparison is not significant and has a p-value greater than 0.05. Therefore, the data comparison suggests that there is no relationship between the two groups and is due to chance. The HFHFD group also shows greater amount of intensity than the NCD group on the ATG5 band membrane as well. This may suggest that there is no relationship between the two groups since the p-value is greater than 0.05. Therefore, no conclusion can be drawn on autophagy upregulation in HFD and HFHFD groups. Lastly, the NEKO-HFHFD group shows significant greater amount of intensity than the HFHFD group. This data comparison is significant since the p-value is less than 0.05. This data comparison may suggest upregulation of autophagy, at least autophagosome formation, when neutrophil elastase is knocked out in HFHFD group. This further supports the hypothesis that autophagy, in order to protect cells and maintain homeostasis, is increased in the NEKO-HFHFD group.

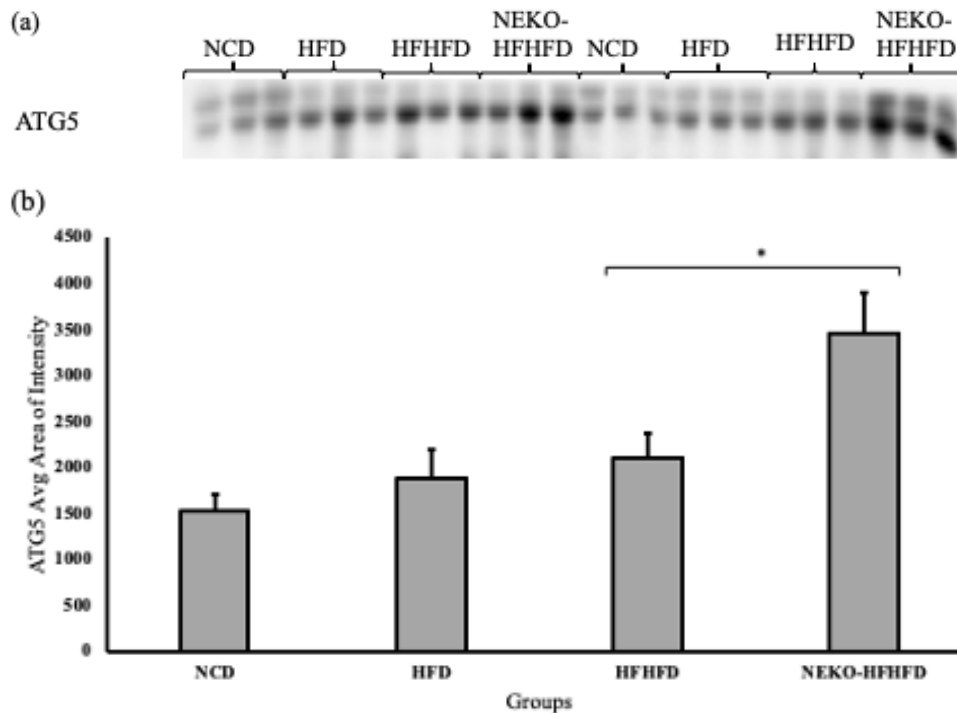


Figure 5. ATG5 Western Blot Data. 25 μ L of each sample from each group loaded onto gel. The sample groups include NCD, HFD, HFHFD, NEKO-HFHFD from mice sample collected on 07/26/19. The primary antibody, ATG5, is from Cell Signaling and is Rabbit antibody (1:1000 dilution). (a) shows ATG5 membrane in the four different groups. (b) shows quantified measurement of ATG5 membrane based on average area of intensity for each group. * $p \leq 0.05$ based on two-tailed t-test

Vimentin is an intermediate filament and a fibrosis marker. As shown in figure 6, the liver samples from NCD and HFD groups have no difference in vimentin protein levels. However, the HFHFD group shows greater amount of intensity compared to the NCD group. Statistically, the two groups are significantly different since the p-value is less than 0.05. Therefore, it is possible that fibrosis is increased in HFHFD group. Data obtained by other members in our lab support this conclusion. Lastly, the NEKO-HFHFD group shows significant less amount of vimentin protein than the HFHFD group. This

data comparison is significant since the p-value is less than 0.05 and supports the notion that NEKO mice are resistant to diet-induced liver fibrosis. This data comparison may suggest upregulation of autophagy upstream leading to less fibrosis in the NEKO-HFHFD group. The HFHFD group (i.e. when NE is not knocked out) shows greater amount of intensity on the Vimentin antibody which may suggest that autophagy might not be functioning properly or there is another upstream issue in HFHFD group.

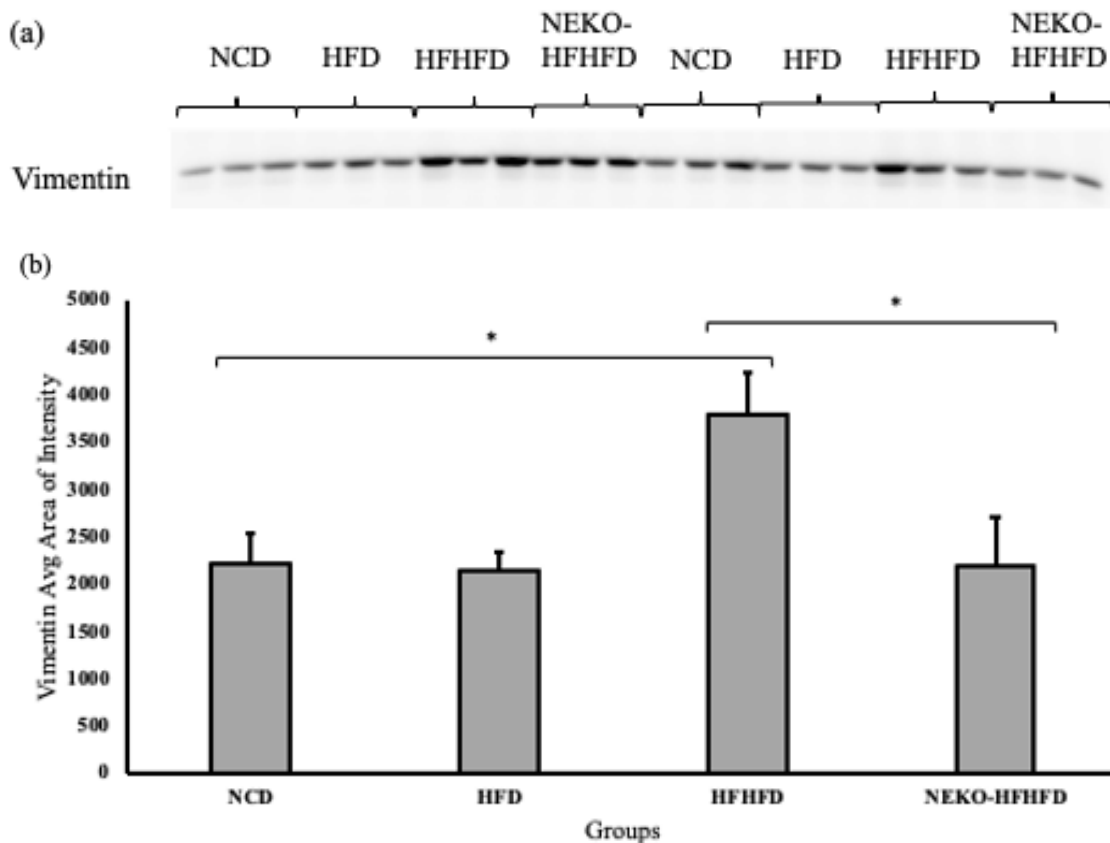


Figure 6. Vimentin Western Blot Data. 35 μ L of each sample from each group loaded onto gel. The sample groups include NCD, HFD, HFHFD, NEKO-HFHFD from mice sample collected on 07/26/19. The primary antibody, Vimentin, is from Cell Signaling and is Rabbit antibody (1:1000 dilution). (a) shows Vimentin membrane in the four different groups. (b) shows quantified measurement of Vimentin membrane based on average area of intensity for each group. * $p \leq 0.05$ based on two-tailed t-test

DISCUSSION

In brief recap, obesity has become a worldwide issue as calorie intake exceeds calorie burn-off. Increase in prevalence of obesity in the population, increases the risk of liver diseases such as NAFLD. The progression of NAFLD can lead to NASH and, eventually to an irreversible step, cirrhosis. Benign liver injury is not an issue; however, more chronic liver injury, as in the case of NAFLD, can lead to overexposure to the immune system, which can cause damaging effects to the liver. The increased levels of neutrophils, and therefore neutrophil elastase, in the liver can cause liver cells to become dysfunctional. Likewise, autophagy has been known to provide protection to the body by getting rid of harmful and leftover substances in cells in order to maintain cellular homeostasis. The autophagy pathway begins with upstream signaling from master regulators such as AMPK and mTOR. Next, a phagophore is formed from other organelles in the body such as the ER or Golgi. After further activation by the ULK1 complex and PI3K complex, an autophagosome can be assembled. LC3 and ATG complex are then required in order for the autophagosome to be completely assembled. The final steps include a lysosome fusing with the autophagosome. This creates the autolysosome, which will then degrade and recycle the material that was engulfed earlier from the cytosol. There are also specific kinds of autophagy such as mitophagy and lipophagy which are important in mitochondrial and lipid maintenance in the body. However, for the purposes of this thesis, the main focus was on the autophagy pathway.

Furthermore, in order to explain this protective phenomenon several western blot experiments were completed using liver samples collected from four different mice

models. The four conditions were WT-NCD, WT-HFD, WT-HFHF, and NEKO-HFHF. Although any conclusion for determining autophagy upregulation when neutrophil elastase is knocked out for protective effects or in certain diet group for maintenance effects, some suggestions can be made for further investigation. Based on the results, p-ULK1 (S317), LC3-II, and ATG5 showed significantly higher levels of intensity in the NEKO-HFHF group when compared to the HFHF group. This does suggest that the autophagy pathway was activated and significantly upregulated when neutrophil elastase was knocked out. Also, protein level of vimentin, a biomarker of fibrotic activation in the liver, is also inhibited in NEKO mice. Our data suggested that activation of autophagy pathways in NEKO mice may lead to the protective effect on diet-induced liver fibrosis. Further studies will need in order to reproduce same results and to explain the protective effect seen when NE is not present.

Limitations

Some of the limitations in the experiments and getting the results out was due to technical issues of making sure the bands on the membrane were clear and reliable. Although many primary antibodies were used, not all data and antibodies were able to make it onto to thesis in order to ensure scientific integrity and to place reliable and reproducible data. For example, during the earlier days of running western blots, sometimes the primary antibody for overnight incubation did not fully cover the membrane, which caused uneven amount of primary antibody to spread. This error made the final image of the membrane lopsided with one side of the membrane having a signal

and the other side not having a signal, or at least a weak signal. Another technical issue was making sure the gradient gel actually was a gradient gel. The purpose of the gradient gel is to have the higher concentration, which was 15% concentration of the resolving gel, to be at the bottom while lower concentration, which was the 5% concentration, to be at the top of the gel. Unfortunately, many of the times when the big gel was running, the top portion of the gel didn't produce good results. The top portion of the resolving gel is important for high molecular weight antibodies such as p-mTOR and p-ACC. The p-mTOR antibody was particularly an important marker since it is a master regulator of the autophagy pathway. Another limitation on top of the technical issues was time constraint. Big western blot gels take three days to complete from making the gel to taking images. Every day of those three required patience and delicate skills in order to ensure decent results. If a mistake was made during any of those three days, further delays would ensue. Repetition of the same experiments also put constrain on the sample, since the sample was limited. The experience has been a great learning experience in terms of learning technical skills in the lab but also soft skills such as researching about the antibodies that are being used, how the antibodies connect in the autophagy pathway, and communication skills.

Future Directions

To further move this project along, more cell-signaling pathways will need to be explored and more antibodies will need to be used. For example, one of the pathways that is important in connecting with autophagy and liver disease would be exploring

mitophagy pathway. As mentioned in the introduction, mitophagy is a specific type of autophagy related to the mitochondria, and in order for cells to remain healthy and to control mitochondrial health, mitophagy is stimulated so that the mitochondria can be recycled and can preserve ATP production^[71]. Mitophagy markers that can be further explored are: VDAC1, p62/SQSTM1, PINK1, and Parkin. The other pathway that can be explored to help explain the hypothesis and prove upregulation of autophagy is lipophagy. Lipophagy is another specific type of autophagy that leads to the degradation of intracellular lipid droplets. One of the lipophagy markers to further explore would be LAMP2. LAMP2, as mentioned before, is a component of lysosomal membranes, involved in lysosomal stability, and is another regulator in the autophagy pathway. Another lipophagy marker would be LAL. So, when LDs are engulfed by the lysosome, they are broken down by lipases such as LAL. LALs can catabolize triglycerides and cholesteryl esters. Additionally, more western blots will need to be to solidify data on both those mentioned in this thesis and data that has been mentioned in other studies. Some of those antibodies include p-mTOR, mTOR, p-ACC, ACC, p-PERK, PERK, PARP, p-AMPK, AMPK, p-Beclin1, Beclin1, p-AKT, AKT, PARP alpha, TFEB, Sirt1, Leptin Receptor, Caspase 3, ATG13, p-P70S6K, P70S6K, p-S6RP, and S6RP.

Besides western blots, different sample groups might be used to study this autophagy phenomenon in hepatic stellate cells. Also, tissue staining using immunohistology to further examine tissue morphology changes among groups. Electric microscopy is another direction that can be taken to provide a better visual on organelles in the cell such as mitochondria and lysosomes.

REFERENCES

1. *Obesity and Overweight*. (2020a, April 1). World Health Organization. <https://www.who.int/news-room/fact-sheets/detail/obesity-and-overweight>
2. *Obesity - Symptoms and causes*. (2020, November 18). Mayo Clinic. <https://www.mayoclinic.org/diseases-conditions/obesity/symptoms-causes/syc-20375742#:~:text=Obesity%20is%20a%20complex%20disease,blood%20pressure%20and%20certain%20cancers.>
3. *Obesity and overweight*. (2020b, April 1). World Health Organization. <https://www.who.int/news-room/fact-sheets/detail/obesity-and-overweight>
4. *U.S. Obesity Rate May Hit 42% by 2050*. (2010, November 5). MedicineNet. <https://www.medicinenet.com/script/main/art.asp?articlekey=121732>
5. Estes, C., Razavi, H., Loomba, R., Younossi, Z., & Sanyal, A. J. (2017). Modeling the epidemic of nonalcoholic fatty liver disease demonstrates an exponential increase in burden of disease. *Hepatology*, 67(1), 123–133. <https://doi.org/10.1002/hep.29466>
6. Day, J. A. (2017, May 3). *Diet for Fatty Liver Disease: The Johns Hopkins Digestive Weight Loss Center*. Johns Hopkins Medicine. https://www.hopkinsmedicine.org/endoscopic-weight-loss-program/conditions/fatty_liver_disease.html#:~:text=Non%2Dalcoholic%20fatty%20liver%20disease%20is%20strongly%20associated%20with%20obesity,first%20step%20towards%20developing%20diabetes.
7. *Burden of liver diseases in the world*. (2019, January 1). ScienceDirect. <https://www.sciencedirect.com/science/article/abs/pii/S0168827818323882?via%3Dihub>
8. Li, R., Toan, S., & Zhou, H. (2020). Role of mitochondrial quality control in the pathogenesis of nonalcoholic fatty liver disease. *Aging*, 12(7), 6467–6485. <https://doi.org/10.18632/aging.102972>
9. Ludwig, J. (1980, July). *Nonalcoholic steatohepatitis: Mayo Clinic experiences with a hitherto unnamed disease*. PubMed. <https://pubmed.ncbi.nlm.nih.gov/7382552/>
10. Friedman, S. L. (2003). *Liver fibrosis -- from bench to bedside*. PubMed. <https://pubmed.ncbi.nlm.nih.gov/12591185/>

11. Mendez-Sanchez, N., Cruz-Ramon, V., Ramirez-Perez, O., Hwang, J., Barranco-Fragoso, B., & Cordova-Gallardo, J. (2018). New Aspects of Lipotoxicity in Nonalcoholic Steatohepatitis. *International Journal of Molecular Sciences*, *19*(7), 2034. <https://doi.org/10.3390/ijms19072034>
12. Wick, G., Backovic, A., Rabensteiner, E., Plank, N., Schwentner, C., & Sgonc, R. (2010). The immunology of fibrosis: innate and adaptive responses. *Trends in Immunology*, *31*(3), 110–119. <https://doi.org/10.1016/j.it.2009.12.001>
13. Beaven, S. W., Matveyenko, A., Wroblewski, K., Chao, L., Wilpitz, D., Hsu, T. W., Lentz, J., Drew, B., Hevener, A. L., & Tontonoz, P. (2013). Reciprocal Regulation of Hepatic and Adipose Lipogenesis by Liver X Receptors in Obesity and Insulin Resistance. *Cell Metabolism*, *18*(1), 106–117. <https://doi.org/10.1016/j.cmet.2013.04.021>
14. Mendez-Sanchez, N., Cruz-Ramon, V., Ramirez-Perez, O., Hwang, J., Barranco-Fragoso, B., & Cordova-Gallardo, J. (2018b). New Aspects of Lipotoxicity in Nonalcoholic Steatohepatitis. *International Journal of Molecular Sciences*, *19*(7), 2034. <https://doi.org/10.3390/ijms19072034>
15. Fuchs, M., & Sanyal, A. J. (2012). Lipotoxicity in NASH. *Journal of Hepatology*, *56*(1), 291–293. <https://doi.org/10.1016/j.jhep.2011.05.019>
16. Pierantonelli, I., & Svegliati-Baroni, G. (2019). Nonalcoholic Fatty Liver Disease: Basic Pathogenetic Mechanisms in the Progression From NAFLD to NASH. *Transplantation*, *103*(1), e1–e13. <https://doi.org/10.1097/tp.0000000000002480>
17. Sunny, N. E., Bril, F., & Cusi, K. (2017). Mitochondrial Adaptation in Nonalcoholic Fatty Liver Disease: Novel Mechanisms and Treatment Strategies. *Trends in Endocrinology & Metabolism*, *28*(4), 250–260. <https://doi.org/10.1016/j.tem.2016.11.006>
18. Patterson, R. E., Kalavalapalli, S., Williams, C. M., Nautiyal, M., Mathew, J. T., Martinez, J., Reinhard, M. K., McDougall, D. J., Rocca, J. R., Yost, R. A., Cusi, K., Garrett, T. J., & Sunny, N. E. (2016). Lipotoxicity in steatohepatitis occurs despite an increase in tricarboxylic acid cycle activity. *American Journal of Physiology-Endocrinology and Metabolism*, *310*(7), E484–E494. <https://doi.org/10.1152/ajpendo.00492.2015>
19. Lalor, P., Faint, J., Aarbodem, Y., Hubscher, S., & Adams, D. (2007). The Role of Cytokines and Chemokines in the Development of Steatohepatitis. *Seminars in Liver Disease*, *27*(2), 173–193. <https://doi.org/10.1055/s-2007-979470>

20. Klebanoff, S. J. (2005). Myeloperoxidase: friend and foe. *Journal of Leukocyte Biology*, 77(5), 598–625. <https://doi.org/10.1189/jlb.1204697>
21. Lumeng, C. N., Bodzin, J. L., & Saltiel, A. R. (2007). Obesity induces a phenotypic switch in adipose tissue macrophage polarization. *Journal of Clinical Investigation*, 117(1), 175–184. <https://doi.org/10.1172/jci29881>
22. *Two Types of Macrophages: M1 and M2 Macrophages - Cusabio*. (n.d.). CUSABIO. <https://www.cusabio.com/c-20938.html>
23. Pham, C. T. N. (2006). Neutrophil serine proteases: specific regulators of inflammation. *Nature Reviews Immunology*, 6(7), 541–550. <https://doi.org/10.1038/nri1841>
24. Talukdar, S., Oh, D. Y., Bandyopadhyay, G., Li, D., Xu, J., Mcnelis, J., ... Olefsky, J. M. (2012). Neutrophils mediate insulin resistance in mice fed a high-fat diet through secreted elastase. *Nature Medicine*, 18(9), 1407–1412. <https://doi.org/10.1038/nm.2885>
25. Mansuy-Aubert, V., Zhou, Q., Xie, X., Gong, Z., Huang, J. Y., Khan, A., Aubert, G., Candelaria, K., Thomas, S., Shin, D. J., Booth, S., Baig, S., Bilal, A., Hwang, D., Zhang, H., Lovell-Badge, R., Smith, S., Awan, F., & Jiang, Z. (2013). Imbalance between Neutrophil Elastase and its Inhibitor α 1-Antitrypsin in Obesity Alters Insulin Sensitivity, Inflammation, and Energy Expenditure. *Cell Metabolism*, 17(4), 534–548. <https://doi.org/10.1016/j.cmet.2013.03.005>
26. Ali, M., Jasmin, S., Fariduddin, M., Alam, S. M. K., Arslan, M. I., & Biswas, S. K. (2018). Neutrophil elastase and myeloperoxidase mRNA expression in overweight and obese subjects. *Molecular Biology Reports*, 45(5), 1245–1252. <https://doi.org/10.1007/s11033-018-4279-4>
27. *Autophagy: What You Need to Know*. (2018, August 23). Healthline. <https://www.healthline.com/health/autophagy#benefits>
28. Levine, B., Packer, M., & Codogno, P. (2015). Development of autophagy inducers in clinical medicine. *Journal of Clinical Investigation*, 125(1), 14–24. <https://doi.org/10.1172/jci73938>
29. Gatica, D., Lahiri, V., & Klionsky, D. J. (2018). Cargo recognition and degradation by selective autophagy. *Nature Cell Biology*, 20(3), 233–242. <https://doi.org/10.1038/s41556-018-0037-z>

30. Pickles, S., Vigié, P., & Youle, R. J. (2018). Mitophagy and Quality Control Mechanisms in Mitochondrial Maintenance. *Current Biology*, 28(4), R170–R185. <https://doi.org/10.1016/j.cub.2018.01.004>
31. Galluzzi, L., Baehrecke, E. H., Ballabio, A., Boya, P., Bravo-San Pedro, J. M., Cecconi, F., Choi, A. M., Chu, C. T., Codogno, P., Colombo, M. I., Cuervo, A. M., Debnath, J., Deretic, V., Dikic, I., Eskelinen, E. - L., Fimia, G. M., Fulda, S., Gewirtz, D. A., Green, D. R., ... Kroemer, G. (2017). Molecular definitions of autophagy and related processes. *The EMBO Journal*, 36(13), 1811–1836. <https://doi.org/10.15252/embj.201796697>
32. Mizushima, N., Levine, B., Cuervo, A. M., & Klionsky, D. J. (2008). Autophagy fights disease through cellular self-digestion. *Nature*, 451(7182), 1069–1075. <https://doi.org/10.1038/nature06639>
33. Mijaljica, D., Prescott, M., & Devenish, R. J. (2011). Microautophagy in mammalian cells: Revisiting a 40-year-old conundrum. *Autophagy*, 7(7), 673–682. <https://doi.org/10.4161/auto.7.7.14733>
34. Saftig, P., Beertsen, W., & Eskelinen, E.-L. (2008). LAMP-2: A control step for phagosome and autophagosome maturation. *Autophagy*, 4(4), 510–512. <https://doi.org/10.4161/auto.5724>
35. Carlsson, S. R., & Simonsen, A. (2015). Membrane dynamics in autophagosome biogenesis. *Journal of Cell Science*, 128(2), 193–205. <https://doi.org/10.1242/jcs.141036>
36. Simonsen, A., & Tooze, S. A. (2009). Coordination of membrane events during autophagy by multiple class III PI3-kinase complexes. *Journal of Cell Biology*, 186(6), 773–782. <https://doi.org/10.1083/jcb.200907014>
37. Mizushima, N. (2007). Autophagy: process and function. *Genes & Development*, 21(22), 2861–2873. <https://doi.org/10.1101/gad.1599207>
38. Saxton, R. A., & Sabatini, D. M. (2017). mTOR Signaling in Growth, Metabolism, and Disease. *Cell*, 168(6), 960–976. <https://doi.org/10.1016/j.cell.2017.02.004>
39. Matsunaga, K., Morita, E., Saitoh, T., Akira, S., Ktistakis, N. T., Izumi, T., Noda, T., & Yoshimori, T. (2010). Autophagy requires endoplasmic reticulum targeting of the PI3-kinase complex via Atg14L. *The Journal of Experimental Medicine*, 207(9), i24. <https://doi.org/10.1084/jem2079oia24>

40. Kocaturk, N. M., & Gozuacik, D. (2018). Crosstalk Between Mammalian Autophagy and the Ubiquitin-Proteasome System. *Frontiers in Cell and Developmental Biology*, 6, 128. <https://doi.org/10.3389/fcell.2018.00128>
41. Ohsumi, Y. (2001). Molecular dissection of autophagy: two ubiquitin-like systems. *Nature Reviews Molecular Cell Biology*, 2(3), 211–216. <https://doi.org/10.1038/35056522>
42. Kabeya, Y. (2000). LC3, a mammalian homologue of yeast Apg8p, is localized in autophagosome membranes after processing. *The EMBO Journal*, 19(21), 5720–5728. <https://doi.org/10.1093/emboj/19.21.5720>
43. Pankiv, S., Clausen, T. H., Lamark, T., Brech, A., Bruun, J.-A., Outzen, H., Øvervatn, A., Bjørkøy, G., & Johansen, T. (2007). p62/SQSTM1 Binds Directly to Atg8/LC3 to Facilitate Degradation of Ubiquitinated Protein Aggregates by Autophagy. *Journal of Biological Chemistry*, 282(33), 24131–24145. <https://doi.org/10.1074/jbc.m702824200>
44. Berg, T. O., Fengsrud, M., Strømhaug, P. E., Berg, T., & Seglen, P. O. (1998). Isolation and Characterization of Rat Liver Amphisomes. *Journal of Biological Chemistry*, 273(34), 21883–21892. <https://doi.org/10.1074/jbc.273.34.21883>
45. Dibble, C. C., Elis, W., Menon, S., Qin, W., Klekota, J., Asara, J. M., Finan, P. M., Kwiatkowski, D. J., Murphy, L. O., & Manning, B. D. (2012). TBC1D7 Is a Third Subunit of the TSC1-TSC2 Complex Upstream of mTORC1. *Molecular Cell*, 47(4), 535–546. <https://doi.org/10.1016/j.molcel.2012.06.009>
46. Zhang, Y., Gao, X., Saucedo, L. J., Ru, B., Edgar, B. A., & Pan, D. (2003). Rheb is a direct target of the tuberous sclerosis tumour suppressor proteins. *Nature Cell Biology*, 5(6), 578–581. <https://doi.org/10.1038/ncb999>
47. Avruch, J., Hara, K., Lin, Y., Liu, M., Long, X., Ortiz-Vega, S., & Yonezawa, K. (2006). Insulin and amino-acid regulation of mTOR signaling and kinase activity through the Rheb GTPase. *Oncogene*, 25(48), 6361–6372. <https://doi.org/10.1038/sj.onc.1209882>
48. Bakula, D., Müller, A. J., Zuleger, T., Takacs, Z., Franz-Wachtel, M., Thost, A.-K., Brigger, D., Tschan, M. P., Frickey, T., Robenek, H., Macek, B., & Proikas-Cezanne, T. (2017). WIPI3 and WIPI4 β -propellers are scaffolds for LKB1-AMPK-TSC signalling circuits in the control of autophagy. *Nature Communications*, 8(1), 15637. <https://doi.org/10.1038/ncomms15637>

49. Kim, J., Kundu, M., Viollet, B., & Guan, K.-L. (2011). AMPK and mTOR regulate autophagy through direct phosphorylation of Ulk1. *Nature Cell Biology*, *13*(2), 132–141. <https://doi.org/10.1038/ncb2152>
50. Settembre, C., Zoncu, R., Medina, D. L., Vetrini, F., Erdin, S., Erdin, S. U., Huynh, T., Ferron, M., Karsenty, G., Vellard, M. C., Facchinetti, V., Sabatini, D. M., & Ballabio, A. (2012). A lysosome-to-nucleus signalling mechanism senses and regulates the lysosome via mTOR and TFEB. *The EMBO Journal*, *31*(5), 1095–1108. <https://doi.org/10.1038/emboj.2012.32>
51. Martina, J. A., Chen, Y., Gucek, M., & Puertollano, R. (2012). MTORC1 functions as a transcriptional regulator of autophagy by preventing nuclear transport of TFEB. *Autophagy*, *8*(6), 903–914. <https://doi.org/10.4161/auto.19653>
52. Settembre, C., Zoncu, R., Medina, D. L., Vetrini, F., Erdin, S., Erdin, S. U., Huynh, T., Ferron, M., Karsenty, G., Vellard, M. C., Facchinetti, V., Sabatini, D. M., & Ballabio, A. (2012b). A lysosome-to-nucleus signalling mechanism senses and regulates the lysosome via mTOR and TFEB. *The EMBO Journal*, *31*(5), 1095–1108. <https://doi.org/10.1038/emboj.2012.32>
53. *Strategies to detect mitochondrial oxidants*. (2019, February 1). ScienceDirect. <https://www.sciencedirect.com/science/article/pii/S2213231718309819?via%3Dihub>
54. Zhang, M., Shi, R., Zhang, Y., Shan, H., Zhang, Q., Yang, X., Li, Y., & Zhang, J. (2019). Nix/Bnip3L-dependent mitophagy accounts for airway epithelial cell injury induced by cigarette smoke. *Journal of Cellular Physiology*, *234*(8), 14210–14220. <https://doi.org/10.1002/jcp.28117>
55. Saxena, S., Mathur, A., & Kakkar, P. (2019). Critical role of mitochondrial dysfunction and impaired mitophagy in diabetic nephropathy. *Journal of Cellular Physiology*, *234*(11), 19223–19236. <https://doi.org/10.1002/jcp.28712>
56. Bayne, A. N., & Trempe, J.-F. (2019). Mechanisms of PINK1, ubiquitin and Parkin interactions in mitochondrial quality control and beyond. *Cellular and Molecular Life Sciences*, *76*(23), 4589–4611. <https://doi.org/10.1007/s00018-019-03203-4>
57. Sarraf, S. A., Raman, M., Guarani-Pereira, V., Sowa, M. E., Huttlin, E. L., Gygi, S. P., & Harper, J. W. (2013). Landscape of the PARKIN-dependent ubiquitylome in response to mitochondrial depolarization. *Nature*, *496*(7445), 372–376. <https://doi.org/10.1038/nature12043>

58. Bernardini, J. P., Lazarou, M., & Dewson, G. (2016). Parkin and mitophagy in cancer. *Oncogene*, *36*(10), 1315–1327. <https://doi.org/10.1038/onc.2016.302>
59. Wang, L., Liu, X., Nie, J., Zhang, J., Kimball, S. R., Zhang, H., Zhang, W. J., Jefferson, L. S., Cheng, Z., Ji, Q., & Shi, Y. (2015). ALCAT1 controls mitochondrial etiology of fatty liver diseases, linking defective mitophagy to steatosis. *Hepatology*, *61*(2), 486–496. <https://doi.org/10.1002/hep.27420>
60. Gonçalves, I. O., Passos, E., Diogo, C. V., Rocha-Rodrigues, S., Santos-Alves, E., Oliveira, P. J., Ascensão, A., & Magalhães, J. (2016). Exercise mitigates mitochondrial permeability transition pore and quality control mechanisms alterations in nonalcoholic steatohepatitis. *Applied Physiology, Nutrition, and Metabolism*, *41*(3), 298–306. <https://doi.org/10.1139/apnm-2015-0470>
61. Lübke, T., Lobel, P., & Sleat, D. E. (2009). Proteomics of the lysosome. *Biochimica et Biophysica Acta (BBA) - Molecular Cell Research*, *1793*(4), 625–635. <https://doi.org/10.1016/j.bbamcr.2008.09.018>
62. Carotti, S., Aquilano, K., Zalfa, F., Ruggiero, S., Valentini, F., Zingariello, M., Francesconi, M., Perrone, G., Alletto, F., Antonelli-Incalzi, R., Picardi, A., Morini, S., Lettieri-Barbato, D., & Vespasiani-Gentilucci, U. (2020). Lipophagy Impairment Is Associated With Disease Progression in NAFLD. *Frontiers in Physiology*, *11*, 850. <https://doi.org/10.3389/fphys.2020.00850>
63. Carotti, S., Aquilano, K., Zalfa, F., Ruggiero, S., Valentini, F., Zingariello, M., Francesconi, M., Perrone, G., Alletto, F., Antonelli-Incalzi, R., Picardi, A., Morini, S., Lettieri-Barbato, D., & Vespasiani-Gentilucci, U. (2020b). Lipophagy Impairment Is Associated With Disease Progression in NAFLD. *Frontiers in Physiology*, *11*, 850. <https://doi.org/10.3389/fphys.2020.00850>
64. Feldstein, A. E., Canbay, A., Angulo, P., Taniai, M., Burgart, L. J., Lindor, K. D., & Gores, G. J. (2003). Hepatocyte apoptosis and fas expression are prominent features of human nonalcoholic steatohepatitis. *Gastroenterology*, *125*(2), 437–443. [https://doi.org/10.1016/s0016-5085\(03\)00907-7](https://doi.org/10.1016/s0016-5085(03)00907-7)
65. Wieckowska, A., Zein, N. N., Yerian, L. M., Lopez, A. R., McCullough, A. J., & Feldstein, A. E. (2006). In vivo assessment of liver cell apoptosis as a novel biomarker of disease severity in nonalcoholic fatty liver disease. *Hepatology*, *44*(1), 27–33. <https://doi.org/10.1002/hep.21223>
66. Kucukoglu, O., Guldiken, N., Chen, Y., Usachov, V., El-Heliebi, A., Haybaeck, J., Denk, H., Trautwein, C., & Strnad, P. (2014). High-fat diet triggers Mallory-Denk body formation through misfolding and crosslinking of excess keratin 8. *Hepatology*, *60*(1), 169–178. <https://doi.org/10.1002/hep.27068>

67. Castro, R. E., Ferreira, D. M. S., Afonso, M. B., Borrallho, P. M., Machado, M. V., Cortez-Pinto, H., & Rodrigues, C. M. P. (2013). miR-34a/SIRT1/p53 is suppressed by ursodeoxycholic acid in the rat liver and activated by disease severity in human non-alcoholic fatty liver disease. *Journal of Hepatology*, *58*(1), 119–125. <https://doi.org/10.1016/j.jhep.2012.08.008>
68. Derdak, Z., Villegas, K. A., Harb, R., Wu, A. M., Sousa, A., & Wands, J. R. (2013). Inhibition of p53 attenuates steatosis and liver injury in a mouse model of non-alcoholic fatty liver disease. *Journal of Hepatology*, *58*(4), 785–791. <https://doi.org/10.1016/j.jhep.2012.11.042>
69. Lee, S. J., Yoo, J. D., Choi, S. Y., & Kwon, O.-S. (2014). The expression and secretion of vimentin in the progression of non-alcoholic steatohepatitis. *BMB Reports*, *47*(8), 457–462. <https://doi.org/10.5483/bmbrep.2014.47.8.256>
70. Matsunaga, K., Morita, E., Saitoh, T., Akira, S., Ktistakis, N. T., Izumi, T., Noda, T., & Yoshimori, T. (2010b). Autophagy requires endoplasmic reticulum targeting of the PI3-kinase complex via Atg14L. *The Journal of Experimental Medicine*, *207*(9), i24. <https://doi.org/10.1084/jem2079oia24>
71. Pickles, S., Vigié, P., & Youle, R. J. (2018b). Mitophagy and Quality Control Mechanisms in Mitochondrial Maintenance. *Current Biology*, *28*(4), R170–R185. <https://doi.org/10.1016/j.cub.2018.01.004>

CURRICULUM VITAE

